SWARM Absolute Scalar Magnetometer accuracy: analyses and measurement results

T. Jager, J-M. Léger, and F. Bertrand
CEA-LETI, MINATEC,
17 rue des Martyrs
38054 Grenoble Cedex 9, France
thomas.jager@cea.fr

I. Fratter and J-C. Lalaurie
Centre National d'Etudes Spatiales
18 Avenue Edouard Belin
31401 Toulouse Cedex 9, France

The different factors that affect the SWARM optically pumped Absolute Scalar Magnetometer (ASM) accuracy are reviewed and analyzed. An overall precision of less than 45 pT (1 σ) is reported, which is well under the 300 pT specified for global ASM accuracy.

I. INTRODUCTION

The Swarm mission has been selected by the European Space Agency (ESA) as the 3rd Opportunity mission of the Earth Explorer Program. It consists of a constellation of three satellites dedicated to the most advanced survey of the earth's magnetic field and its temporal evolution. In this framework, the Absolute Scalar Magnetometer (ASM) developed by CEA-LETI and CNES will be flown as the magnetic reference instrument on these satellites. Its performances are therefore crucial for the mission's success. This paper reviews the different factors that affect this optically pumped helium sensor accuracy and presents their respective contributions, with emphasis on the control of the heading errors which are usually one of the poorest characteristics of optically pumped instruments. An overall precision of less than 45 pT (1 σ) is reported, which is well under the 300 pT specified for global ASM accuracy, the remaining disruptions originating from the satellite structure itself.

II. ASM OPERATING PRINCIPLE

The ASM instrument is an optically pumped ^{4}He magnetometer based on an electronic magnetic resonance whose effects are amplified by a laser pumping process [1-2], cf Fig. 1. A fraction of the helium atoms are first excited to the 2^3S_1 metastable state by means of a high frequency discharge. This energy level is split by the static magnetic field B_0 into three Zeeman sublevels. The measurement of B_0 is then performed by exciting and detecting the paramagnetic resonance between the Zeeman sublevels: a radiofrequency field B_{RF} is applied on the ^{4}He gas cell and when its frequency matches the Larmor frequency ω_0 of the Zeeman sublevels (here $\omega_0 = \gamma B_0$, where γ is the ^{4}He gyromagnetic ratio for the 2^3S_1 state) the magnetic resonance occurs and transitions are induced between the sublevels. The ASM can thus be viewed as a magnetic-field-to-frequency converter. However, at thermal equilibrium the sublevels are almost equally populated so that no significant change is induced at resonance. In order to detect it, a selective pumping from one of the Zeeman sublevel to the 2^3P_0 state is performed thanks to a frequency-tuned linearly-polarized laser light. The resulting disequilibrium between the Zeeman sublevels populations amplifies the resonance signal amplitude by several orders of magnitude while the monitoring of the intensity of the laser light transmitted through the ^{4}He cell allows its detection.

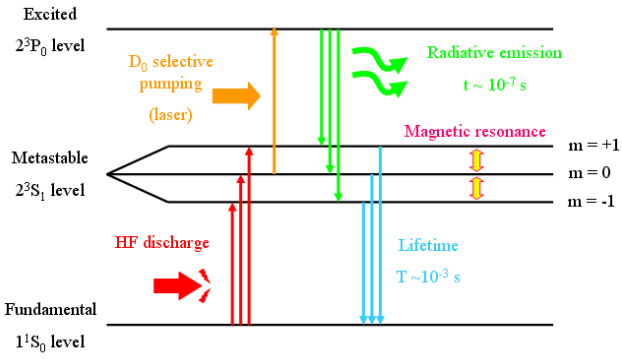

Figure 1. ^{4}He energy diagram and ASM principle of operation

In addition to the high resolution scalar magnetic field measurement a major improvement has been reached with the possibility to derive simultaneously vector measurements with the ASM sensor: 3 low pulsation orthogonal vector modulations are superimposed to the static B_0 field, as detailed in (1), and their projections onto the scalar field are measured.

$$\left\|\vec{B}_{tot}\right\| = \left\|\vec{B}_0 + \sum_{j=1}^{3} \beta^j \cos(\omega_j t)\vec{e}_j\right\| \qquad (1)$$

The additional vector measurement is simply obtained by processing the scalar output measurement containing the principal harmonics at the ω_j pulsations. The vector field reconstruction in the ASM reference frame is finally achieved thanks to a specific calibration process [2] thanks to which the

vector modulation amplitudes β_j and their respective orientations $\boldsymbol{e}_j$ in the ASM frame are derived.

III. ASM HARDWARE

To take full advantage of the scalar magnetometer performances we have defined an architecture that is free of the orientation effects common to all standard scalar magnetometers based on magnetic resonance. Each of the following processes has to be taken into account to guarantee the sensor isotropy:

- the distribution of atoms on the three sublevels 2^3S_1 resulting from the optical pumping cycle is directly dependent on the relative orientation θ_F between the static magnetic field B_0 and the polarization of the laser E_0 (in case of linearly polarized light) or the propagation direction k_0 (in case of circularly polarized light).
- only the component of the radiofrequency field B_{RF} orthogonal to the magnetic field B_0 actually induces resonating transitions between Zeeman sublevels.
- for a linearly polarized pumping beam, the amplitudes of the resonance signals used for the magnetic field B_0 measurement reach an extremum when the polarization direction E_0 is perpendicular to the magnetic field B_0.

We have finally chosen to control the laser beam polarization direction through a rotation of a polarizer placed in front of the ^{4}He cell (linear polarisation) and we have also designed the radiofrequency excitation coils so that the resulting radiofrequency field is parallel to the linear polarizer: whatever the relative orientation of the sensor with respect to the magnetic field direction, both polarisation E_0 and radiofrequency field B_{RF} directions can always be adjusted perpendicularly to the static field B_0. The resulting magnetometer is thus perfectly isotropic and its scalar resolution is independent of the sensor's attitude with respect to the magnetic field direction.

The final instrument assembly is depicted on Fig. 2 and consists of an electronic box, the Digital Processing Unit (DPU), and a separately installed sensor mostly made of PEEK connected to the DPU by optical and electrical harnesses. Given the ASM's critical role, ESA has decided to opt for a full cold redundancy, so that each of the three Swarm satellites will include two complete ASMs: a specific sensor bracket has thus been designed to mechanically interface two identical sensors at the tip of the satellite boom, each sensor being connected to a dedicated DPU located within the satellite main body.

IV. ASM PERFORMANCES

A. Scalar bandwidth and resolution

Compared to the Overhauser based scalar sensors previously used for the Ørsted and CHAMP missions [3], the scalar resolution, which is completely independent of the ambient magnetic field modulus B_0, has been enhanced to 1 pT/√Hz and the scalar bandwidth previously limited to few Hz can be increased up to 300 Hz (set to 100 Hz for the SWARM mission).

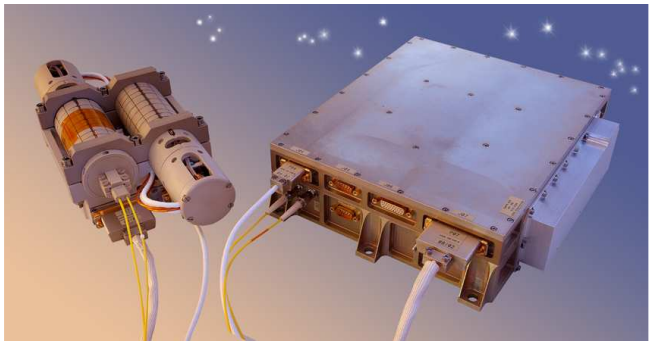

Figure 2. ASM sensor assembly, harnesses and DPU

B. Intrinsic vector resolution

The main objective of the ASM is to provide high resolution scalar measurements for the calibration of the Vector Fluxgate Magnetometer (VFM) developed by the Danish National Space Center. However and as previously mentioned, the ASM will also be able to provide and to demonstrate additional vector measurements from his own. Its vector resolution is by design lower than the one provided by the VFM instrument: the ASM vector measurement resolution is in the 1 nT/√Hz range [2] with a vector measurement bandwidth set to 0.4 Hz.

C. Scalar accuracy

Here is the second major improvement on scalar performances with respect to the previous NMR magnetometers developed by CEA-LETI for space applications. The specific ASM errors affecting the scalar magnetic field measurement have been identified and characterized, as detailed in the followings paragraphs. They can all be corrected on the ASM level1b data thanks to dedicated algo1b algorithms, excepted for the measurement datation and the reference time accuracy errors which are intrinsic random errors.

1) ASM sensor anisotropy

The ASM sensor anisotropy has been demonstrated to be the main instrument related error: while the ASM sensor is only sensitive to the magnetic field modulus and should therefore not depend on the sensor attitude, residual magnetism of the sensor head components leads to heading related errors. It is due on the one hand to the magnetic susceptibility of its materials (e.g. PEEK polymer whose magnetic susceptibility χ is about -5.10^{-6} S.I.) and on the other hand to remaining ferromagnetic signatures of the different ASM sensor components.

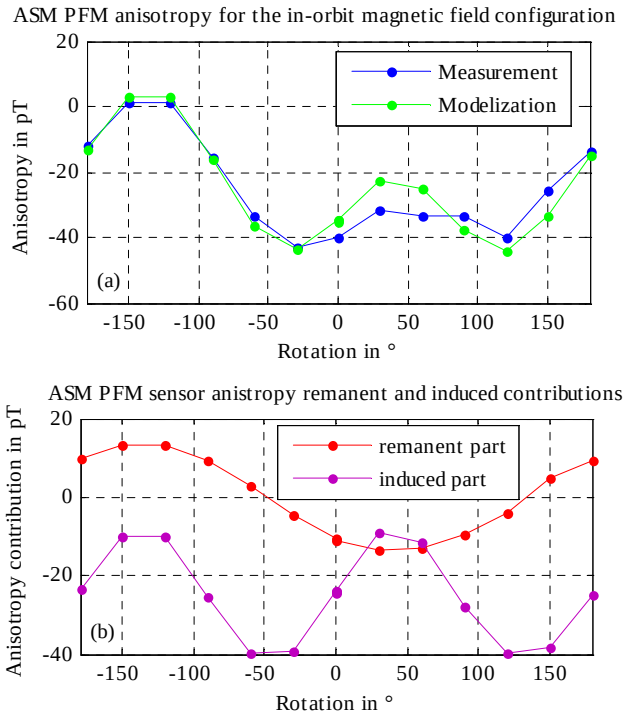

Figure 3. (a) ASM PFM sensor anisotrpoy measurement and corresponding modelization, (b) corresponding remanent and induced contributions of the corrective modeling

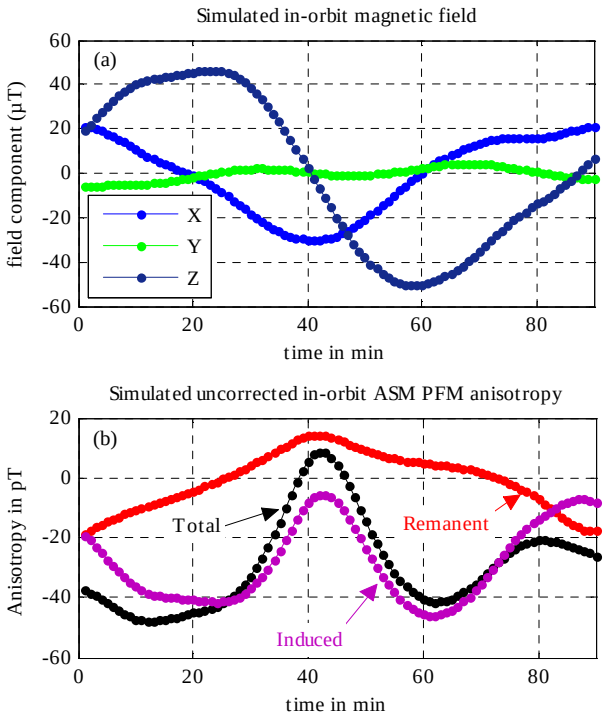

Figure 4. Simulated in-orbit magnetic field (a) and corresponding anisotropy before correction (b)

A tri-axis demagnetization process is applied to minimize the remanent contribution of the ASM sensor components on the anisotropy. The final signature of the ASM sensor isotropy is then measured for the in-orbit magnetic field configuration. For the Proto Flight Model (PFM) sensor, a 45 ± 2.5 pT peak-to-peak signature has been measured as detailed on Fig. 3a. This signature is then corrected with an algorithm taking into account both remanent and induced magnetic contributions as depicted on both graphs of Fig. 3a and Fig. 3b. A final remaining anisotropy error can then be deduced: for the ASM PFM, the remaining mean anisotropy error is of -1.2 pT (maximum peak-to-peak value of 17.2 pT and standard deviation of 5.3 pT).

From the previous anisotropy measurements, we can also deduce the uncorrected anisotropy signature of the ASM PFM sensor along one representative SWARM orbit (before correction in the ASM algo1b algorithms). An illustration of the corresponding simulated anisotropy is given on Fig. 4a and Fig 4b.

2) Vector modulation aliasing

When operated in vector mode, a scalar aliasing is generated by the vector modulations injected on the ASM sensor vector coils. The resulting error on the scalar magnetic field measurement depends on the amplitude of the vector modulations b_m and on the ambient magnetic field modulus B_0. It is given by:

$$\Delta B_{aliasing} = \frac{b_m^2}{2B_0} \qquad (2)$$

It is equal to 25 pT with a 50 nT vector modulation amplitude and an ambient magnetic field of 50 µT. This aliasing error has been measured at different ambient magnetic field values and the analytic description formula has thus been verified within a ± 2.5 pT measurement uncertainty. This deterministic error is also corrected in the algo1b algorithms of the ASM instrument.

3) Bloch-Siegert effect

The Bloch-Siegert effect [4] is a frequency pulling effect towards low-field that introduces a field measurement error inversely proportional to the ambient field modulus. It is given by:

$$\Delta B_{Bloch-Siegert} = -\frac{k_{BS} B_{RF}^2}{B_0}, \qquad (3)$$

where k_{BS} is equal to 1 for ^{4}He (this value has been confirmed during functional ASM performance tests). With B_{RF} equal to 50 nT and an ambient magnetic field value of 50 µT, this error is here of 50 pT. It has also been experimentally determined and the analytic description formula has thus been verified within a ± 2.5 pT measurement uncertainty. This error is also corrected in the algo1b algorithms.

Error type	Bloch-Siegert error	Vector aliasing	ASM in-orbit anisotropy	PPS precision (5.10-7 x B0) (worst case)	Datation (1 ms x 30 nT/s) (worst case)
Initial uncorrected ASM error	50 pT (@ 50 µT)	25 pT (@ 50 µT)	45 pT	32,5 pT (@ 65 µT)	30 pT
Remaining error after ASM level 1B algorithm correction	< 5 pT	< 5 pT	< 5 pT	32,5 pT (@ 65 µT) (system error, not corrected in the level 1b algorithms)	30 pT (instrument error, not corrected at level 1b)

TABLE I. ASM ERRORS CONTRIBUTIONS ON THE SCALAR MEASUREMENT

4) Measurement datation error

The measurement datation error is an error introduced by the ASM instrument measurement sampling rate. The ASM internal B_0 measurement rate is 1 kHz, so that a maximum datation error of 1 ms (corresponding to an rms error of 0.29 ms for a Poisson distribution law) can occur between the measured magnetic field and its corresponding in-orbit localization: given a maximum in-orbit scalar magnetic field variation rate of 30 nT/s, the corresponding maximum error is of 30 pT (the corresponding rms error is of 8.7 pT). Contrary to the previous deterministic errors, the datation error cannot be corrected in the algo1b algorithms.

5) Pulse Per Second (PPS) time reference accuracy

The scalar magnetic field measurement is made through the Larmor frequency determination which depends on an internal reference frequency that is measured every second between each pulse of the PPS signal. Nominally set to 1s, the period of the PPS pulses is guaranteed with a precision of 5.10^{-7}. The corresponding maximum scalar magnetic error measurement is thus directly given by this precision: for a magnetic field of 65 µT (worst case), the corresponding error is of 32.5 pT. As for the measurement datation error, this error cannot be corrected in the algo1b algorithms.

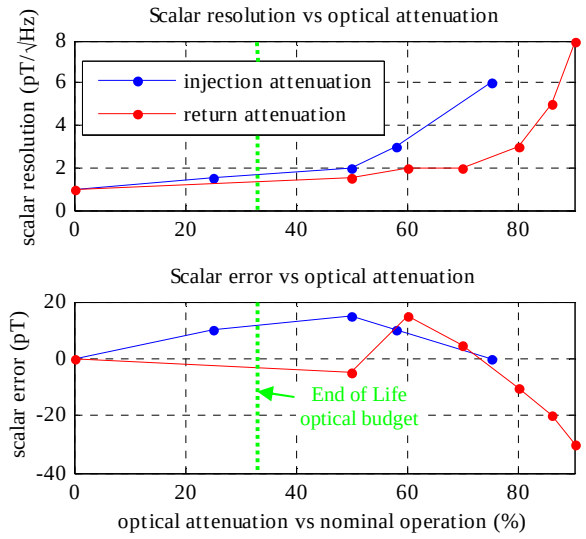

Figure 5. ASM performances vs optical losses

A summary of all scalar measurement errors that have been previously detailed is given in Table 1. Given these figures, the norm of the residual error after level 1b corrections σ_{max} is about 45 pT which is much lower than the global ASM scalar error budget of 300 pT.

Additional error contributions such as the satellite magnetic moment and the magnetocoupler effect will be corrected at satellite level with the SWARM satellite level 1b algorithms.

D. End of life

The ASM instrument has been designed and qualified for the 4.25 years of the SWARM mission. The level of the ASM metrological performances have thus to be kept all along. The ASM scalar resolution and the ASM scalar accuracy will mainly be affected by the evolution of the optical losses in the ASM instrument, and their respective estimated evolutions have been measured by simulating additional optical losses in the instrument. The corresponding results, summarized in Fig. 5, show that no significant degradation will occur over the instrument lifetime: even for the End of Life optical budget (i.e. 33 % of optical attenuation) the scalar resolution is only slightly increased from 1 to 1.5 pT/√Hz., and a maximum 15 pT accuracy error is generated.

V. CONCLUSION AND PERSPECTIVES

The CEA-LETI has successfully designed and fabricated an optically pumped ^{4}He magnetometer which provides absolute scalar magnetic field measurements with a 1 pT/√Hz resolution over a DC to 100 Hz bandwidth. An in-depth analysis, supported by extensive characterization tests, has identified the various factors affecting the magnetometer accuracy which has been demonstrated to be better than 45 pT (norm of the maximum residual error). All ASM flight models are currently being qualified and will be available for the SWARM satellites integration in the coming months.

[1] F. D. Colegrove and P. A. Franken, "Optical Pumping of Helium in the $^3S_1$ Metastable State", Physical Review, vol. 119, 1961, pp. 680–690.

[2] O. Gravrand, A. Khokhlov, J. L. Le Mouël and J. M. Léger., "On the calibration of a vectorial 4He pumped magnetometer", Earth Planets Space, 53, 2001, pp. 949–958.

[3] D. Duret, J-M. Léger, M. Francès, J. Bonzom, F. Alcouffe, A. Perret, J. C. Llorens and C. Baby, "Performances of the OVH magnetometer for the danish Ørsted satellite", IEEE Trans. Magn., 32, 1996, pp. 4935–4937.

[4] F. Bloch and A. Siegert , "Magnetic Resonance for Nonrotating Fields", Physical Review, vol. 57, 1940, pp. 522-527.